Dichloro(bis[diphenylthiourea])cadmium complex as a precursor for HDA-capped CdS nanoparticles and their solubility in water

Authors:
Poslet M. Shumbula[1]
Makwena J. Moloto[2]
Tshinyadzo R. Tshikhudo[3]
Manuel Fernandes[1]

Affiliations:
[1]School of Chemistry, University of the Witwatersrand, South Africa

[2]Department of Chemical Technology, University of Johannesburg, South Africa

[3]Mintek – Advanced Materials Division, Randburg, South Africa

Correspondence to:
Makwena Moloto

email:
mmoloto@uj.ac.za

Postal address:
Department of Chemical Technology, University of Johannesburg, PO Box 17011, Doornfontein 2028, South Africa

Keywords:
cadmium complex; crystal structure; diphenylthiourea; nanoparticles; water-soluble

Dates:
Received: 21 Aug. 2009
Accepted: 07 June 2010
Published: 06 Aug. 2010

How to cite this article:
Shumbula PM, Moloto MJ, Tshikhudo TR, Fernandes M. Dichloro (bis[diphenylthiourea]) cadmium complex as a precursor for HDA-capped CdS nanoparticles and their solubility in water. S Afr J Sci. 2010;106(7/8), Art.#311, 7 pages. DOI: 10.4102/sajs.v106i7/8.311

This article is available at:
http://www.sajs.co.za

ABSTRACT

A single-source precursor route has been explored by using the diphenylthiourea cadmium complex as the source of cadmium sulphide (CdS) nanoparticles. The reaction was carried out using hexadecylamine (HDA) as the solvent and stabilising agent for the particles. The phenylthiourea complex was synthesised and characterised by means of a combination of spectroscopic techniques, microanalysis and X-ray crystal structural analysis. The diphenylthiourea complex was thermolysed in HDA at 120 °C for 1 h to produce CdS nanoparticles. The CdS nanoparticles prepared were made water-soluble via a ligand exchange reaction involving the use of pyridine to displace HDA. The pyridine was, in turn, replaced by glucose and glucuronic acid. The absorption and emission spectra showed the typical features of quantum confinement for the nanoparticles for both HDA-capped and glucose- or glucuronic acid-capped CdS nanoparticles. The change in the capping groups, from HDA to glucose and glucuronic acid, resulted in absorption and emission features that were almost similar, with only slight red-shifting and tailing.

INTRODUCTION

Thiourea and its alkyl derivatives are important precursors for the preparation of metal sulphide nanoparticles. Besides focusing on the applications of these ligands, special attention has been placed on their coordination chemistry to different metal atoms because of the various potential donor sites that these ligands possess.[1] Rosenheim and Meyer[2] reported the complexation of Fe(II) with thiourea and concluded that the coordination was through the sulphur atom, using infrared spectroscopy and X-ray diffractions to determine the coordination. In addition, complexes prepared using the alkyl thiourea, such as methylthiourea, showed, using infrared spectroscopy, that the coordination also was through sulphur.[3] Thiourea and its derivatives were used as a source of sulphur because their advantages in this regard are that they are stable for a long time, easy to synthesise, inexpensive and yield good quality crystalline semiconductor particles.

Semiconductor nanoparticles, which are also known as quantum dots (QDs) or nanocrystals, are small clusters of atoms of a length in the range of 1 nm – 100 nm. They exhibit properties that are different from those of the bulk/macrocrystalline material.[4] Some of the fundamental factors (related to size of the individual nanocrystal) that distinguish semiconductor nanoparticles from their corresponding macrocrystalline material are, (1) a high dispersity (large surface-to-volume ratio) associated with the particles, with both physical and chemical properties of the semiconductor being particularly sensitive to surface structure and (2) the actual size of the particle, which can determine the electronic and physical properties of the material.[5] Over the past decades, semiconductor nanoparticles have been found to be an interesting subject in both research and technical applications, because of their unique size-dependent optical and electronic properties. Scientists worldwide are interested in the quantum size effect[6,7] and the promising applications of semiconductor nanoparticles therein, through their use in light-emitting diodes, solar cells, biological labelling and diagnostic, catalysis, photovoltaic devices and lasers.[8,9] The most significant aspect of the research and manipulation of semiconductor nanoparticles lies in the synthesis of high-quality nanocrystals with a uniform shape and size.

In the past decades, researchers have extensively been studying efficient synthetic routes to well-defined nanocrystals with controlled size and shape. Their methods include gas-phase syntheses utilising vapour-liquid-solid,[10,11] chemical vapour deposition[12,13] and thermal evaporation[14] methods, as well as liquid phase colloidal syntheses in aqueous[15,16] or nonhydrolytic media.[17] A lot of research has been done on metal sulphide nanoparticles, such as cadmium sulphide (CdS), with various compositions and shapes.[18] However, it remains a challenge to synthesise anisotropic-shaped CdS nanocrystals with controllable shape and size in the quantum confinement range, because the preparation of high quality 1D CdS nanorods in this size range is still difficult to achieve through common methods (the diameters of the nanorods or nanowires prepared by common methods are usually beyond 10 nm). Moreover, it is always a goal of nanochemistry to indentify safer, more cost-effective, high-yielding and more controllable methods of nanoparticle synthesis.[19]

Semiconductor nanoparticles are good materials to use as biolabels because of their small size, emission tunability, lower sensitivity to environmental changes and lower rates of photo-degradation, all of which allow for effective long-term experiments. However, in order to make them useful for that application, semiconductor nanoparticles with high water solubility, biocompatibility and photo-stability must be synthesised.[20] Ligand exchange procedures are then capable of converting hydrophobic semiconductor nanoparticles into water-soluble nanoparticles. The new ligand should possess a functionality that is reactive toward the surface atoms of the particle at one end and a water-compatible functionality at the other end.[21] It is known that native QDs made up of semiconductor nanoparticles are toxic in nature. For example, it has been observed that CdSe QDs are highly toxic to cells exposed to UV for a long time, as UV dissolves the CdSe, thereby releasing toxic cadmium ions.[22] However, toxicity did not prevent scientists from looking at biological applications. For example, Hu et al.[23] synthesised CdTe for cancer marker detection. To minimise toxicity, a non-toxic capping agent is recommended.

METHODS

Materials and instrumentation

The precursor, $Cd\{[(C_6H_5NH)_2CS]_2\}Cl_2$ (complex 1), was prepared using a method outlined below. Tri-*n*-octylphosphine oxide (TOPO), hexadecylamine (HDA) and tri-*n*-octylphosphine (TOP) were purchased from Aldrich (Johannesburg, South Africa) and used without further purification. Cadmium chloride, diphenylthiourea, chloroform, toluene, ethanol, methanol, dimethylformamide, pyridine, ethyl acetate and diethyl ether were used as purchased also from Aldrich (Johannesburg, South Africa) to prepare the precursor and CdS nanoparticles. Glucose and glucuronic acid, which were obtained from Aldrich, were used as capping agents for the water-soluble semiconductor nanoparticles. Microanalysis was performed on a CARLO ERBA elemental analyser for carbon, hydrogen, nitrogen and sulphur and infrared spectra were recorded by a Bruker Optics Tensor 27 (Bruker, Ettlingen, Germany). Optical absorption measurements were carried out using a SPECORD 50 UV-visible spectrophotometer (Analytikjena, Jena, Germany) and the photoluminescence spectra were recorded on a PerkinElmer LS 45 fluorescence spectrometer (United Scientific, Johannesburg, South Africa) with a Xenon lamp at room temperature. Particle size and shape were determined by a Tecnai G^2 Spirit electron microscope (FEI, Eindhoven, the Netherlands) operating at 120 kV. The samples were prepared by spreading a drop of dilute dispersion of the as-prepared products on copper grids, which were then dried in air. X-ray diffraction (XRD) analysis was carried out on a Philips X'Pert materials research diffractometer using secondary graphite monochromated Cu Kα radiation (λ = 1.5406 Å) at 40 kV/50 mA. Samples were supported on glass slides. Measurements were taken using a glancing angle of incidence detector at an angle of 2°, for 2θ values over 10° – 80° in steps of 0.05°, with a scan speed of 0.01° 2θ/s. Thermogravimetric analyses (TGA) were carried out using a Perkin Elmer TGA 4000, (Beaconsfield, UK) in the temperature range 50°C – 900 °C under a nitrogen atmosphere at a heating rate of 20 °C/min.

X-ray crystallography

Intensity data were collected on a Bruker APEX II CC D area detector diffractometer with graphite monochromated Mo K_α radiation (50 kV, 30 mA) using the *APEX 2* data collection software.[24] The collection method involved ω-scans of width 0.5° and 512 × 512 bit data frames. Data reduction was carried out using the program *SAINT+* [25] and absorption corrections carried out using *SADABS*.[25] The crystal structure was solved by direct methods using *SHELXTL*.[26] Non-hydrogen atoms were first refined isotropically, which was followed by anisotropic refinement by full matrix least-squares calculations based on F^2 using *SHELXTL*. Hydrogen atoms were first located in the difference map and then positioned geometrically and allowed to ride on their respective parent atoms. Diagrams and publication material were generated using *SHELXTL*, *PLATON* [27] and *ORTEP*-3.[28]

Synthesis of $Cd\{[(C_6H_5NH)_2CS]_2\}Cl_2$ (complex 1)

A hot solution of diphenylthiourea (9.96 g, 4.36 mmol) in ethanol (20 mL) was added to a solution of cadmium chloride (4.0 g, 2.18 mmol) in ethanol (20 mL). The colourless solution turned yellow after 20 min and was vigorously stirred for 2 h under reflux, followed by hot filtration of the solution to remove unreacted materials. The filtrate was stored in a refrigerator (-4 °C) overnight to give yellow crystals. The crystals formed were then filtered and dried; the yield obtained was 5.56 g (57%). Analytical calculations for $C_{26}H_{24}N_4S_2CdCl_2$ were C, 48.80; H, 3.78; N, 8.76; S, 10.02. Found: C, 48.74; H, 3.56; N, 8.89; S, 9.91, while the Fourier transform infrared spectroscopy (FTIR, cm^{-1}) was: 3328 (medium), 1594 (medium), 1535 (strong), 1450 (strong), 1284 (strong), 1025 (medium), 940 (medium), 755 (medium), 689 (very strong).

Synthesis of HDA-capped CdS nanoparticles

Owing to the higher temperature and toxicity of cadmium and the other organic compounds used, the experiment was performed in a fume hood. HDA (5 g) was heated to 120 °C under an inert atmosphere. The precursor (complex 1) was dispersed in 5 mL of TOP in varying amounts (0.5 g, 1 g or 2 g) and then quickly added into the hot HDA solution under stirring, which caused the temperature of the reaction mixture to drop by about 15 °C – 20 °C. Heating was continued to recover the temperature to 120 °C and then the reaction was maintained for 1 h. The solution was then cooled to approximately 70 °C and an excess amount (60 mL) of methanol was added. The flocculent precipitate formed was centrifuged and the supernatant was decanted, after which the isolated solid was dispersed in toluene. The above centrifugation and isolation procedure was then repeated three times for the purification of the prepared CdS nanoparticles.

Glucose- and glucuronic acid-capped CdS nanoparticles

In preparation of glucose- or glucuronic acid-capped CdS nanoparticles, about 1 g of HDA-capped CdS nanomaterials was added to 5 mL of pyridine. The mixture was heated to 40 °C while vigorously stirring for 1 h. After cooling to room temperature, hexane was added to precipitate the nanoparticles that were isolated by centrifugation. The supernatant was then decanted. A glucose or glucuronic acid solution in methanol was added to have an effect on ligand exchange between the glucose or glucuronic acid and pyridine, which had already displaced the HDA. The mixture was then heated for 1 h at 40 °C and run overnight at room temperature. Chloroform and ethyl acetate were added to precipitate the nanoparticles, followed by the addition of diethyl ether for drying the nanoparticles. The resulting product was centrifuged and the solid product isolated for analysis.

RESULTS AND DISCUSSION

Synthesis of dichloro[bis(1,3-diphenyl-2-thiourea)]cadmium (complex 1)

The complex was synthesised similarly to other alkylthiourea metal complexes reported by Moloto et al.[29] The reaction involved $CdCl_2$ and $(C_6H_5NH)_2CS$ in a 1:2 mole ratio in ethanol to produce the complex. A good yield of the yellow crystalline product was obtained; it was found to be air- and moisture-stable and was analysed by a combination of elemental analyses and spectroscopic techniques.

Description of the structure of complex 1

Single crystals of complex 1 suitable for X-ray analysis were obtained from recrystallisation of the respective compound from ethanol at -15 °C. Crystallographic data of complex 1 is represented in Table 1, while selected bond lengths and bond angles are shown in Table 2. The molecular drawing of complex 1 is given in Figure 1. Complex 1 crystallises in the triclinic crystal system with a centre of symmetry and is monomeric in nature. The cadmium complex contains the central atom in a distorted tetrahedral geometry, the edges of which are shared by two sulphur atoms of the diphenylthiourea and two chlorine atoms of the metal source. The two thiourea units are *trans* to each other. The Cd1-Cl1, Cd1-Cl2, Cd1-S1 and Cd1-S2 bond distances are 2.4438(4) Å, 2.4233(4) Å, 2.5511(4) Å and 2.5588(4) Å, respectively. Both thiourea groups are tilted to different sides, resulting in different degrees, displaying Cl1-Cd1-S1-C1 and Cl1-Cd1-S2-C14 torsion angles of 69.74(6) and -177.41(6), respectively. The bite angle of the diphenylthiourea ligand is 108.522(15). The Cd-S bonds, 2.5511(4) and 2.5588(4), are longer than in the N-ethylthiourea complex reported by Moloto et al.[27], which suggests that the δ-bond character of this bond is weak. The C-S (1.7142[16]) and C-N (1.3322[6]) bonds in diphenylthiourea ligands show intermediate character between a single and a double bond length. These bond distances/lengths are in good agreement with those on the thiourea molecules reported in the Cambridge structural database (CSD) by Allen et al.[30], that is, 1.726 Å (C-S) and 1.322 Å (C-N).

Characterisation of CdS nanoparticles

Figure 2 shows the absorption spectra of CdS nanoparticles capped by HDA at different monomer concentration (i.e.

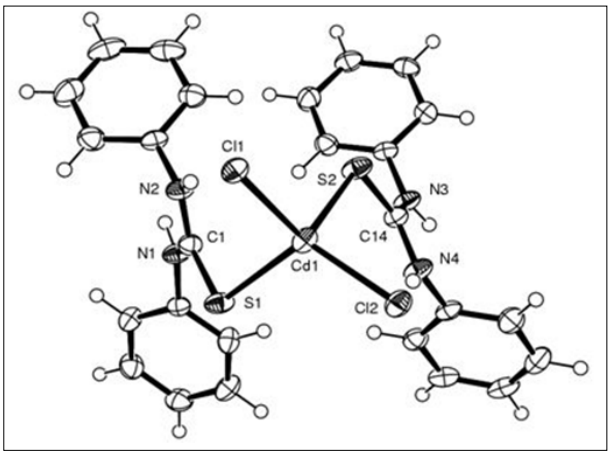

FIGURE 1
Molecular structure of complex 1, where thermal ellipsoids are drawn at the 50% probability level

TABLE 1
Crystal data and structure refinement for complex 1

Description of data	Values and units
Empirical formula	C26 H24 Cd Cl2 N4 S2
Formula weight	639.91 g/mol
Temperature	173(2) K
Wavelength	0.71073 Å
Crystal system	Triclinic
Space group	P-1
Unit cell dimensions	a = 7.7236(2) Å, α = 100.3210(10)°
	b = 11.5115(3) Å, β = 95.5730(10)°
	c = 15.5004(3) Å, γ = 94.9430(10)°
Volume	1341.87(6) Å^3
Z	2
Density (calculated)	1.584 Mg/m^3
Absorption coefficient	1.191 mm^{-1}
F(000)	644
Crystal size	0.40 mm^3 × 0.26 mm^3 × 0.12 mm^3
Absorption correction	Semi-empirical from equivalents
Maximum and minimum transmission	0.8703 and 0.6472
Goodness-of-fit on F^2	1.072
Final *R* indices [*I* > 2sigma(I)]	*R*1 = 0.0214, w*R*2 = 0.0534
R indices (all data)	*R*1 = 0.0238, w*R*2 = 0.0546

The 'a', 'b' and 'c' are the international IUPAC symbols used for the unit cell dimensions to describe a triclinic crystal or any other system.
All the units given in the table, such as *F, Z, R, I, F*(000), are the crystallographic standard symbols used in every table of crystallographic data.

TABLE 2
Bond distances and angles for complex 1

Bond	Distance (Å)
Cd(1)-Cl(2)	2.4233(4)
Cd(1)-Cl(1)	2.4438(4)
Cd(1)-S(1)	2.5511(4)
Cd(1)-S(2)	2.5588(4)
C(14)-S(2)	1.7098(16)
C(1)-S(1)	1.7187(15)
C(1)-N(1)	1.3299(19)
C(1)-N(2)	1.333(2)
C(14)-N(3)	1.329(2)
C(14)-N(4)	1.337(2)

Bond	Angle (°)
Cl(2)-Cd(1)-Cl(1)	122.087(14)
Cl(2)-Cd(1)-S(1)	114.813(14)
Cl(1)-Cd(1)-S(1)	101.268(14)
Cl(2)-Cd(1)-S(2)	103.162(14)
Cl(1)-Cd(1)-S(2)	106.330(14)
S(1)-Cd(1)-S(2)	108.522(15)
C(1)-S(1)-Cd(1)	98.66(5)
C(14)-S(2)-Cd(1)	104.12(5)

0.5 g, 1 g and 2 g). The absorption spectra were recorded at room temperature by dispersing the particles in toluene. The absorption band edges for HDA-capped CdS nanoparticles increased slightly as the monomer concentration increased, appearing at 458 nm (2.71 eV, Figure 2a), 464 nm (2.67 eV, Figure 2b) and 474 nm (2.62 eV, Figure 2c). These values indicate blue shifts of about 57 nm (Figure 2a), 51 nm (Figure 2b) and 41 nm (Figure 2c) from the bulk CdS (515 nm). These shifts signify the finite size of the nanoparticles, because as the size of the particles decreases, band gap energy increases. All the HDA-capped CdS nanoparticles were prepared at 120 °C for 1 h. For water-soluble CdS nanoparticles, glucose and glucuronic acid were employed as the capping agents after displacing HDA.

Figure 3 shows the absorption spectra of water-soluble CdS nanoparticles capped by: glucose from 0.5 g of complex 1 to 5 g HDA (Figure 3a), glucose from 1 g of complex 1 to 5 g HDA (Figure 3b), glucuronic acid from 2 g of complex 1 to 5 g HDA (Figure 3c) and glucose from 2 g of complex 1 to 5 g HDA (Figure 3d). These spectra, which are also blue-shifted to the bulk CdS, show some tailing when compared to those of the nanoparticles that were HDA-capped, which indicates either the formation of larger particles or particle aggregation. The band edges of the water-soluble CdS nanoparticles were also slightly higher than those capped by HDA, which can be attributed to the ligand exchange, which involved the use of pyridine before incorporation of the sugar molecules.

The photoluminescence spectra of HDA-capped CdS nanocrystals

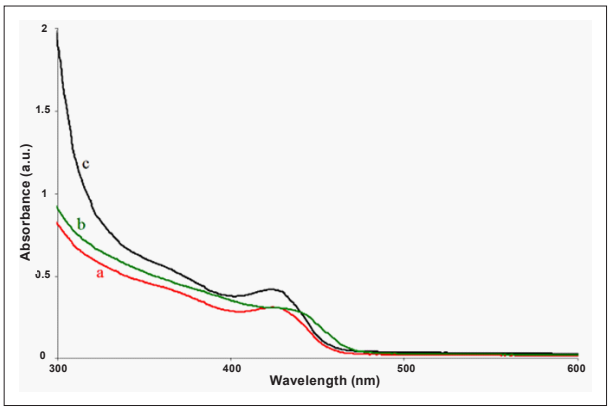

The amounts of complex 1 used to achieve these absorption spectra are, (a) 0.5 g, (b) 1 g and (c) 2 g.

FIGURE 2
Absorption spectra of cadmium sulphide nanoparticles capped by 5 g hexadecylamine with different amounts of complex 1

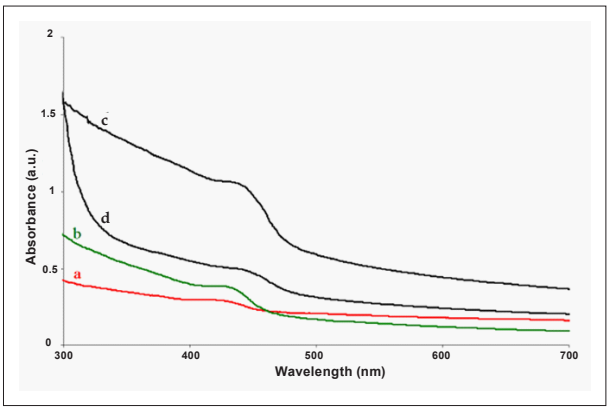

Absorption spectra of CdS nanocrystals capped by glucose of particles obtained from, (a) 0.5 g of complex 1 in 5 g hexadecylamine (HDA), (b) 1 g of complex 1 in 5 g HDA, (c) 2 g of complex 1 in 5 g HDA and (d) glucuronic acid of particles obtained from 2 g of complex 1 in 5 g HDA.

FIGURE 3
Absorption spectra of cadmium sulphide (CdS) nanoparticles capped by glucose and glucuronic acid

at different monomer concentrations are shown in Figure 4. These concentrations were 0.5 g (Figure 4a), 1 g (Figure 4b) and 2 g (Figure 4c). All the spectra that are red-shifted to their as-prepared absorption spectra (Figure 2) show a slight shift to lower energy as the monomer concentration was increased. This conforms to the observed features in the absorption spectra. The narrow emission peaks (Figures 4a and 4b) and the broad peak (Figure 4c) were positioned at 436 nm, 448 nm and 461 nm, respectively. The emission spectra of CdS nanoparticles capped by glucose and glucuronic acid (shown in Figures 5a-5d) appeared at higher wavelengths (lower energy) when compared to the emission spectra of CdS nanoparticles capped by HDA. Their maximum absorption peaks were positioned at 453 nm (Figure 5a), 464 nm (Figure 5b) and 482 nm (Figures 5c and 5d). Similar trends were observed when glucuronic acid was used instead of glucose in the ligand exchange process.

Transmission electron microscopy (TEM) images of HDA-capped CdS nanoparticles at different monomer concentrations of 0.5 g, 1 g and 2 g are shown in Figures 6a–6c, respectively; short rods were mostly observed, with average diameters of 2.4 nm, 3.6 nm and 4.8 nm, respectively. As the precursor concentration was increased from 0.5 g to 2 g, traces of spherical particles were observed. An increase in diameter of the particle size as the monomer concentration increased confirms the results obtained above from the absorption and emission spectra. Figure 7 depicts TEM images of CdS nanoparticles capped by: glucose from 0.5 g of complex 1 to 5 g HDA (Figure 7a), glucose from 1 g of complex 1 to 5 g HDA (Figure 7b), glucuronic acid from 2 g of complex 1 to 5 g HDA (Figure 7c) and glucose from 2 g of complex 1 to 5 g HDA (Figure 7d). No significant changes were observed between the particles capped by HDA and those capped by glucose or glucuronic acid, with the exception of the fine edges being lost on the surface of nanoparticles and some aggregation of the particles, especially in the glucuronic acid-capped CdS nanoparticles (Figure 7d). FTIR spectral analysis of HDA-capped CdS nanoparticles, as seen in Figure 8a, showed C-N and C-H stretching vibrations at 1469 cm^{-1} and 2850 cm^{-1} – 2915 cm^{-1}, respectively. The N-H asymmetric peak at 3318 cm^{-1} was very weak because the amine group on the HDA molecule was bound to the surface of the nanocrystal. Similar observations were also reported by Meulenberg et al.[31] Broad bands of valence (symmetrical and asymmetrical) oscillations of OH at 3368 cm^{-1} and C-H at 2847 cm^{-1} were due to the presence of glucuronic acid (Figure 8b), while another broad band of OH appearing at 3230 cm^{-1} was due to glucose (Figure 8c). The well-defined band appearing at 1709 cm^{-1} corresponds to the valence vibration of the carbonyl group.

The crystallinity of the prepared CdS nanoparticles was investigated by XRD, as shown in Figure 9. It is interesting to find that the pattern of the CdS nanoparticles capped by HDA (2 g of complex 1 in 5 g HDA) sample can be indexed to the

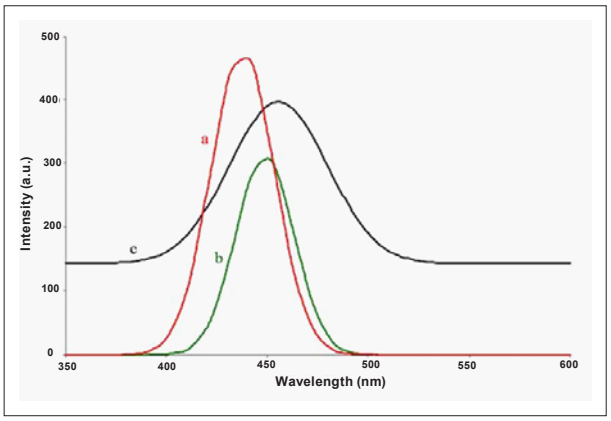

The amounts of complex 1 used to achieve these photoluminescence spectra were, (a) 0.5 g, (b) 1 g and (c) 2 g.
λ_{exc} = 250 nm

FIGURE 4
Photoluminescence spectra of cadmium sulphide nanoparticles capped by 5 g hexadecylamine with different amounts of complex 1

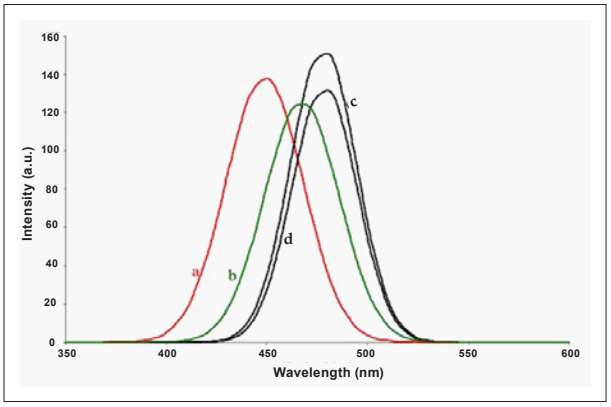

Photoluminescence spectra of CdS nanoparticles capped by glucose of particles obtained from, (a) 0.5 g of complex 1 in 5 g hexadecylamine (HDA), (b) 1 g of complex 1 in 5 g HDA, (c) 2 g of complex 1 in 5 g HDA and (d) glucuronic acid of particles obtained from 2 g of complex 1 in 5 g HDA.

FIGURE 5
Photoluminescence spectra of cadmium sulphide (CdS) nanoparticles capped by glucose and glucuronic acid

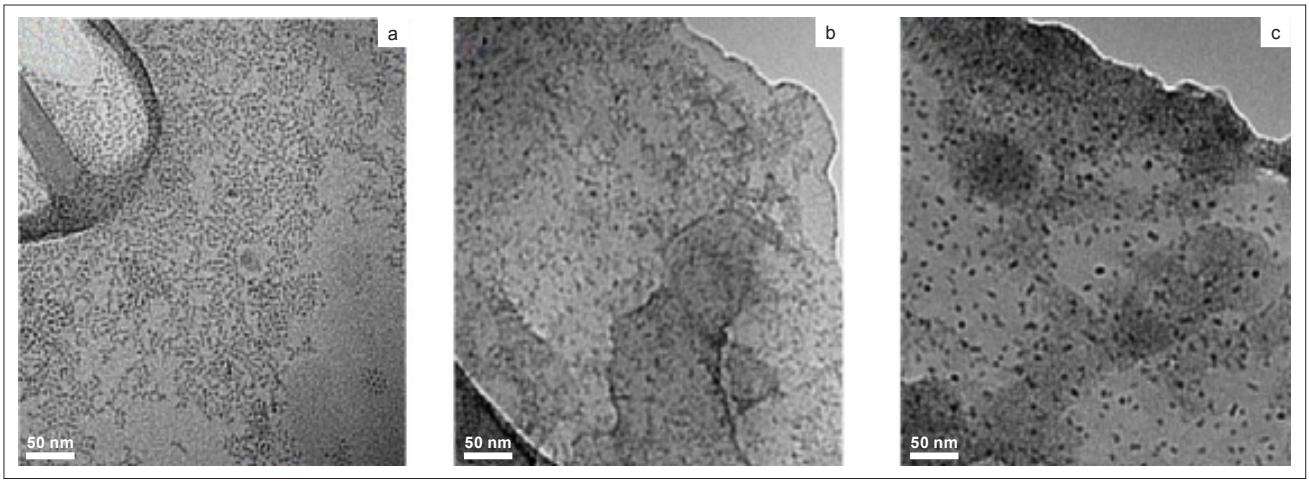

The amounts of complex 1 used were, (a) 0.5 g, (b) 1 g and (c) 2 g.

FIGURE 6
Transmission electron microscopy (TEM) images of cadmium sulphide nanoparticles coated by 5 g hexadecylamine with different amounts of complex 1

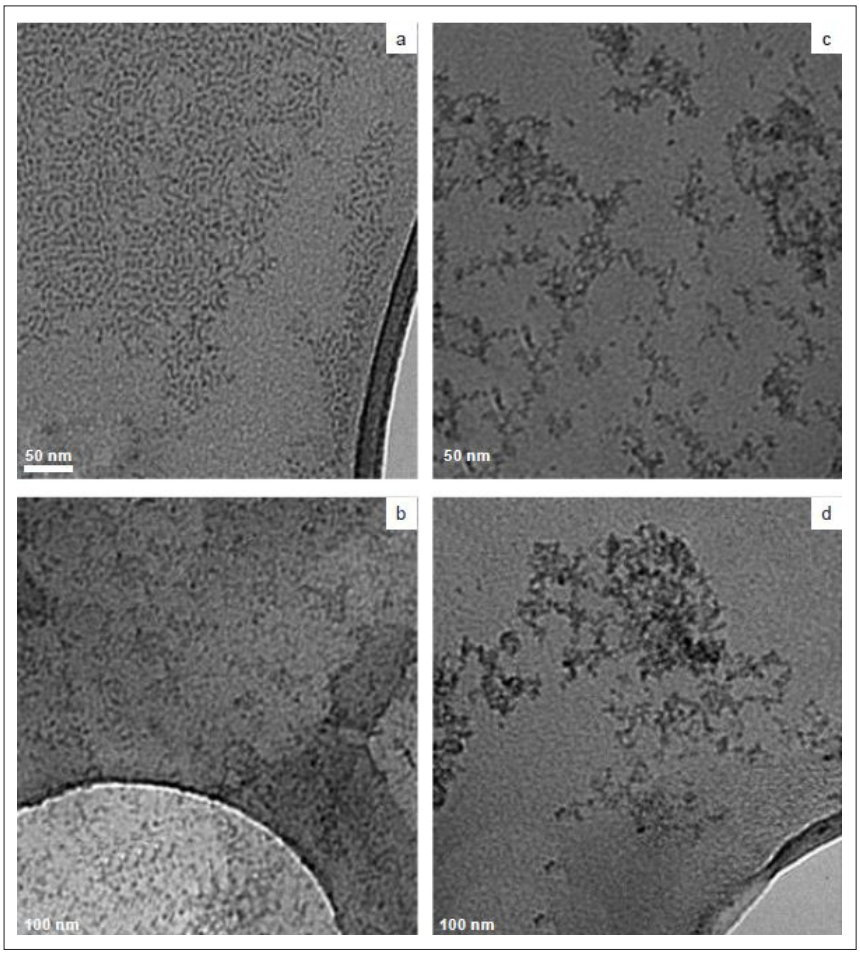

CdS nanoparticles coated by glucose, obtained from (a) 0.5 g of complex 1 in 5 g hexadecylamine (HDA), (b) 1 g of complex 1 in 5 g HDA, (c) 2 g of complex 1 in 5 g HDA and (d) CdS nanoparticles coated by glucuronic acid, obtained from 2 g of complex 1 in 5 g HDA.

FIGURE 7
Transmission electron microscopy (TEM) images of cadmium sulphide (CdS) nanoparticles coated by glucose and glucuronic acid

hexagonal phase, with predominant peaks indexed to 002, 102, 110, 103 and 112. The XRD peaks are considerably broader than those of the macrocrystalline CdS, which signifies the finite size of the particles. In Figure 9, the peak marked with an asterisk was due to the presence of the capping agent (HDA). Figures 10 and 11 show the XRD patterns of CdS nanoparticles capped by glucuronic acid and glucose, respectively. XRD could not reveal the crystallinity of the CdS nanoparticles because multiple peaks were present due to the crystalline sugar molecules being in the same region as the CdS materials. A small amount of HDA-capped CdS nanoparticles synthesised from 0.5 g and 1 g of the precursor was obtained after precipitation and this resulted in even smaller fractions being transferred into the sugars, making XRD analysis difficult.

TGA curves (Figure 12) showed a single step decomposition pattern of the glucose- and glucuronic acid-capped CdS nanoparticles. The onset of decomposition was at a temperature of 189 °C and 198 °C for glucuronic acid and glucose, respectively. The curve below 100 °C indicates the absence of water in the glucose and glucuronic acid CdS nanoparticles. For CdS nanoparticles capped with glucuronic acid, a steady loss was observed at a temperature range of 168 °C – 315 °C, with a weight loss of 57%, while glucose-capped CdS nanoparticles showed a weight loss of about 80% at a temperature range of 197 °C – 402 °C. Both glucose and glucuronic acid gave a residue of 18% and 23%, respectively. HDA-capped CdS nanoparticles showed an immediate mass loss, due to the use of solvents such as toluene and methanol, followed by two subsequent losses, resulting in approximately 10% residue at a temperature of about 378 °C.

CONCLUSION

The absorption spectra of CdS nanoparticles capped with different capping agents were blue-shifted to the bulk CdS, with the emission spectra being red-shifted to the as-prepared CdS particles. The tailing of the absorption spectra of glucuronic acid- and glucose-capped CdS nanoparticles and the emission maxima are an indication of slight difference in the size of the particles, which was also confirmed by TEM. Most interesting was the use of pyridine in the ligand exchange reaction, which

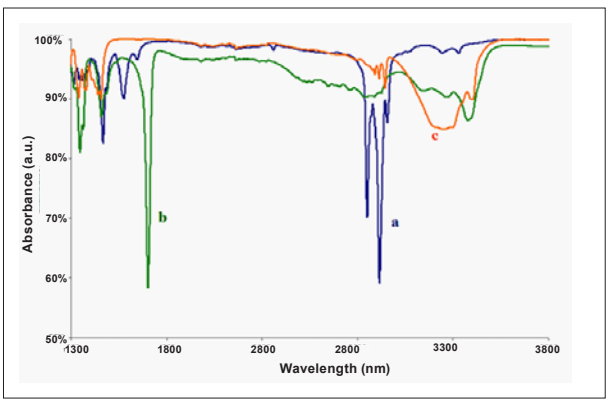

FIGURE 8
Fourier transform infrared spectra of cadmium sulphide nanoparticles capped with, (a) hexadecylamine, (b) glucuronic acid and (c) glucose

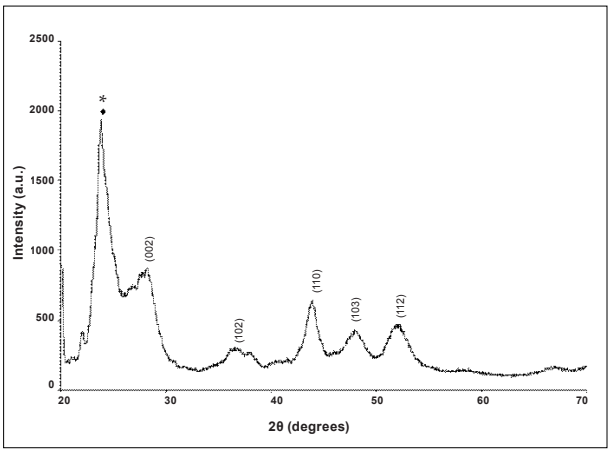

*This peak was due to the presence of HDA as the capping agent

FIGURE 9
Powder X-ray diffraction patterns of hexadecylamine (HDA)-capped cadmium sulphide nanoparticles (2 g of complex 1 in 5 g HDA) synthesised at 120 °C

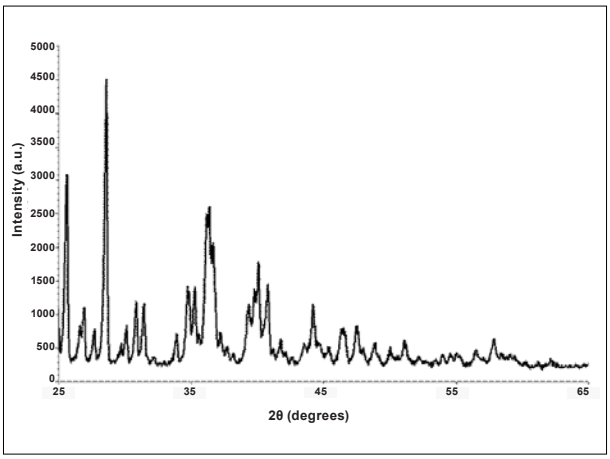

FIGURE 11
Powder X-ray diffraction patterns of glucose-capped cadmium sulphide (CdS) nanoparticles synthesised from hexadecylamine (HDA)-capped CdS (2 g of complex 1 in 5 g HDA) at room temperature

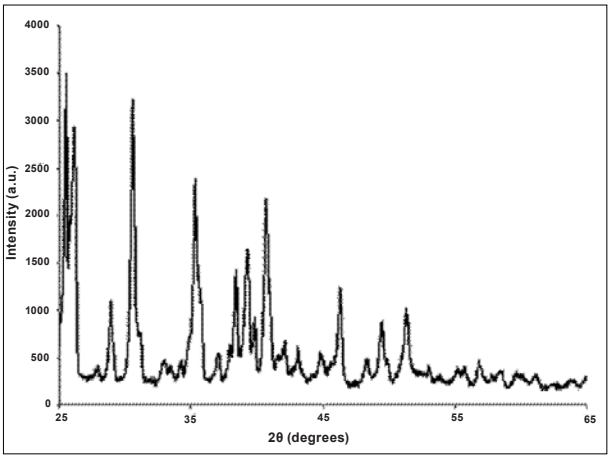

FIGURE 10
Powder X-ray diffraction patterns of glucuronic acid-capped cadmium sulphide (CdS) nanoparticles synthesised from hexadecylamine (HDA)-capped CdS (2 g of complex 1 in 5 g HDA) at room temperature

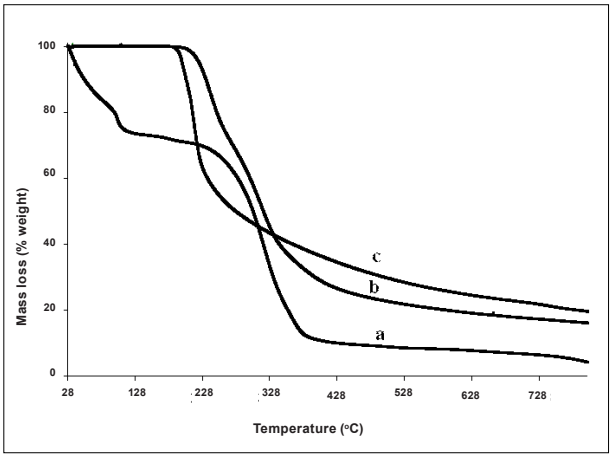

FIGURE 12
Thermogravimetric analysis curves for cadmium sulphide nanoparticles capped with (a) hexadecylamine, (b) glucose and (c) glucuronic acid

cleanly and successfully made the particles soluble in water, without changing the particle shapes. FTIR spectral analysis confirmed the complete removal of HDA from the surface of the nanoparticles.

ACKNOWLEDGEMENTS

This work was supported by funding from the South African National Research Foundation, the University of the Witwatersrand and National Department of Science and Technology/Mintek (NIC). The work was carried out in the research laboratories of the School of Chemistry at the University of the Witwatersrand.

REFERENCES

1. Moloto MJ, Revaprasadu N, O'Brien P, Malik MA. N-Alkylthioureacadmium (II) complexes as novel precursors for the synthesis of CdS nanoparticles. J Mater Sci Mater Electron. 2004;15:313–316.
2. Rosenheim A, Meyer VJZ. [Bonding of thiocarbamates to divalent metal salt]. Z Anorg Chem. 1906;49:13–27. German.
3. Bailey RA, Peterson TR. Some complexes of Fe(II) with thiourea ligands. Can J Chem. 1967;45:1135–1142.
4. Nair PS, Radhakrishinan T, Revaprasadu N, Kolawole GA, O'Brien P. Cd($NH_2CSNHNHCSNH_2$)Cl_2: A new single-source precursor for the preparation of CdS nanoparticles. Polyhedron. 2003;22:3129–3135.
5. Trindade T, O'Brien P, Pickett NL. Nanocrystalline semiconductors: Synthesis, properties, and perspectives. Chem Mater. 2001;13:3843–3858.
6. Chestnoy N, Hull R, Brus LE. Higher excited electronic states in clusters of ZnSe, CdSe, and ZnS: Spin-orbit, vibronic, and relaxation phenomena. J Chem Phys. 1986;85:2237–2242.
7. Alivisatos AP. Semiconductor clusters, nanocrystals, and quantum dots. Science. 1996;271:933–937.
8. Achermann M, Petruska MA, Kos S, Smith DL, Koleske DD, Klimov VI. Energy-transfer pumping of semiconductor nanocrystals using an epitaxial quantum well. Nature. 2004;429:642–646.
9. Allivisatos AP. The use of nanocrystals in biological detection. Nat Biotechnol. 2004;22:47–52.
10. Hu J, Odom TW, Lieber CM. Chemistry and physics in one dimension: Synthesis and properties of nanowires and nanotubes. Acc Chem Res. 1999;32:435–445.
11. Xia X, Yang P, Sun Y, et al. One-dimensional nanostructures: Synthesis, characterization, and applications. Adv Mater. 2003;15:353–389.
12. Duan X, Lieber CM. General synthesis of compound semiconductor nanowires. Adv Mater. 2000;12:298–302.
13. Goldberger J, He R, Zhang Y, et al. Single-crystal gallium nitride nanotubes. Nature. 2003;422:599–602.
14. Pan ZW, Dai ZR, Xu L, Lee ST, Wang ZL. Temperature-controlled growth of silicon-based nanostructures by thermal evaporation of SiO powders. J Phys Chem B. 2001;105:2507–2514.

15. Pileni MP. II-VI semiconductors made by soft chemistry: Synthesis and optical properties. Catal Today. 2000;58:151–166.
16. Steigerwald ML, Allivisatos AP, Gibson JM, et al. Surface derivatization and isolation of semiconductor cluster molecules. J Am Chem Soc. 1988;110:3046–3050.
17. Puntes VF, Krishnan KM, Allivisatos AP. Colloidal nanocrystal shape and size control: The case of cobalt. Science. 2001;291:2115–2117.
18. Jun Y, Jung Y, Cheon J. Architectural control of magnetic semiconductor nanocrystals. J Am Chem Soc. 2002;124:615–619.
19. Li Y, Li X, Yang C, Li Y. Controlled synthesis of CdS nanorods and hexagonal nanocrystals. J Mater Chem. 2003;13:2641–2648.
20. Fan H, Leve EW, Scullin C, et al. Surfactant-assisted synthesis of water-soluble and biocompatible semiconductor quantum dot micelles. Nano Lett. 2005;5:645–648.
21. Chan WCW, Nie S. Quantum dot bioconjugates for ultrasensitive nonisotopic detection. Science. 1988;281:2016–2018.
22. Chan WCW, Maxwell DJ, Bailey RE, Han M, Nie S. Luminescent QDs for multiplexed biological detection and imaging. Curr Opin Biotechnol. 2002;13:40–46.
23. Hu F, Ran Y, Zhou Z, Gao M. Preparation of bioconjugates of CdTe nanocrystals for cancer marker detection. Nanotechnology. 2006;17:2972–2977.
24. APEX2 [computer program]. Version 2.0-1. Madison: Bruker AXS Inc.; 2005.
25. SAINT+ [computer program]. Version 6.0 (includes XPREP and SADABS). Madison: Bruker AXS Inc.; 2005.
26. SHELXTL [computer program]. Version 5.1 (includes XS, XL, XP, XSHELL). Madison: Bruker AXS Inc.; 2005.
27. Spek AL. Single-crystal structure validation with the program PLATON. J Appl Cryst. 2003;36:7–13.
28. Farrugia LJ. ORTEP-3 for Windows – A version of ORTEP-III with a Graphical User Interface (GUI). J Appl Cryst. 1997;30:565–566.
29. Moloto MJ, Malik MA, O'Brien P, Motevalli M, Kolawole GA. Synthesis and characterisation of some *N*-alkyl/aryl and *N*,*N*′-dialkyl/aryl thiourea cadmium(II) complexes: The single crystal X-ray structures of $[CdCl_2(CS(NH_2)NHCH_3)_2]_n$ and $[CdCl_2(CS(NH_2)NHCH_2CH_3)_2]$. Polyhedron. 2003;22:595–603.
30. Allen FH, Kennard O, Watson DG, Brammer L, Orpen AG, Taylor R. In: Wilson AJC, editor. International Tables of Crystallography. Mathematical, Physics and Chemical Tables, Vol. C. Dordrecht: Kluwer Publishers, 1991; p. 685–706.
31. Meulenberg RW, Bryan S, Yun CS, Strouse GF. Effects of alkylamine chain length on the thermal behavior of CdSe quantum dot glassy films. J Phys Chem B. 2002;106:7774–7780.

South African Journal of Science Article #311